Limnol. Oceanogr., 44(4), 1999, 1056–1071

Odor transport in turbulent flows: Constraints on animal navigation

Christopher M. Finelli[1]
Marine Science Program, Belle W. Baruch Institute for Marine Biology and Coastal Research, University of South Carolina, Columbia, South Carolina 29208

N. Dean Pentcheff
Department of Biological Sciences, Belle W. Baruch Institute for Marine Biology and Coastal Research, University of South Carolina, Columbia, South Carolina 29208

Richard K. Zimmer-Faust
Department of Biology, University of California, Box 951606, Los Angeles, California 90095-1006

David S. Wethey
Marine Science Program, Department of Biological Sciences, Belle W. Baruch Institute for Marine Biology and Coastal Research, University of South Carolina, Columbia, South Carolina 29208

Abstract

Odor plumes are common features of aquatic and terrestrial environments, forming an olfactory landscape through which animals must navigate to locate resources and avoid potential hazards. Time-averaged concentration profiles suggest that plumes consist of stable gradients in odor that animals may use for orientation. However, the time scales necessary to generate such profiles are much longer than those typically associated with the neural or behavioral components of odor-mediated search. In contrast, plume measurements made at biologically relevant scales have indicated that turbulent plumes consist of discrete odor filaments separated by clean water. In addition, certain characteristics of individual odor filaments may vary consistently with distance from the odor source, thus providing directional information to a navigating organism. Unfortunately, there is no method to predict the distribution of these putative chemical cues, and our knowledge of odor dispersal is limited to very few laboratory flume studies. Here, we present the results of a field study during which we measured the distributions of the time-averaged concentration, properties of odor filaments, conditional statistics, and relevant hydrodynamic mixing parameters. Many of the observed odor plume characteristics have similar spatial distributions through a range of hydrodynamic conditions. The high degree of similarity in the distribution of many odor plume characteristics suggests that organisms can rely on any number of metrics to successfully orient in an odor plume. However, the temporal and spatial scales of odor dispersal may constrain the strategies used by navigating organisms and influence the efficiency of odor-mediated search. These field results should provide the basis for further empirical and theoretical work on chemosensory-mediated behavior of aquatic animals.

Olfaction is one of the most commonly used sensory systems for navigation and communication (Dusenbury 1992). The chemical cues used in olfaction are released from a wide variety of sources that can be active (i.e., odors are intentionally released for communication purposes) or passive (i.e., odors are the byproduct of processes such as respiration or disturbance). Plumes of these dissolved compounds make up the olfactory landscape (Nevitt et al. 1995; Atema 1996), a dynamic sensory environment used by animals in a number of important ecological interactions. For example, in marine systems, odors are used in mating (Atema and Engstrom 1971; Beach et al. 1975; Gleeson 1980), foraging (Mathewson and Hodgson 1972; Kleerekoper et al. 1975; Rittschof 1980, 1992; Sloan and Northway 1982; Brown and Rittschof 1984; Himmelman 1988; Valentincic 1991; Weissburg and Zimmer-Faust 1993, 1994), and habitat selection (Zimmer-Faust and Spanier 1987; Sweatman 1988; Woodin 1991; Pawlik 1992; Boudreau et al. 1993). These examples highlight the range of taxa (crustaceans, gastropods, echinoderms, fish), habitats (abyssal, estuarine, temperate coastal, tropical reef), and ontogenetic stages (larval, juvenile, adult) for which olfactory-mediated behavior has been demonstrated.

[1] Present address: Patrick Center for Environmental Research, Academy of Natural Sciences, 1900 Benjamin Franklin Parkway, Philadelphia, Pennsylvania 19103-1195.

Acknowledgments

We thank Dennis Allen and the rest of the Baruch Staff for providing facilities and logistic support for this project. J. E. Eckman, T. J. Hilbish, P. A. Jumars, S. A. Woodin, and an anonymous reviewer made useful comments on earlier versions of this manuscript. We especially thank M. Weissburg for his help in clarifying the operation of olfactory neurons with respect to odor pulses. This work is supported by NSF grant IBN 92-2225 to D.S.W. and R.K.Z., grants from the National Academy of Sciences through Sigma Xi, the Lerner-Grey Fund for Marine Research, and the Slocum-Lunz Foundation to C.M.F., and fellowships from the Belle W. Baruch Institute for Coastal Research and Marine Biology, the University of South Carolina Graduate School, and the University of South Carolina Marine Science Program to C.M.F. This article is contribution 1176 of the Belle W. Baruch Institute for Marine Biology and Coastal Research.

An organism's ability to orient to an odor plume depends on the temporal and spatial distribution of odorant in the water column. Water motion, and therefore odor dispersal, is dominated by turbulence for the vast majority of habitats and macroorganisms (Denny 1993; Vogel 1994). Subsequently, organisms detect chemical cues when the turbulent plume contacts sensory structures carried internally (e.g., in gill chambers) or externally on the body surface (e.g., on antennae or legs). Thus, the temporal and spatial distribution of odor molecules in the plume interacts with the temporal and spatial resolution of sensory arrays to determine the olfactory signal delivered to an organism for processing by the nervous system.

The dispersal of odor plumes has been studied extensively over the last 40 yr. Early attempts to describe odor concentration profiles using the statistical Gaussian distribution assumed homogeneous mixing of odor within the plume (Wright 1958; Crisp and Meadows 1962; Bossert and Wilson 1963). However, these workers also recognized that rapid fluctuations in concentration tended to overwhelm such time-averaged Gaussian concentration distributions at short temporal scales (Wright 1958; Bossert and Wilson 1963). The use of fast ion detectors in terrestrial habitats (Murlis and Jones 1981) and conductivity (Moore and Atema 1988), fast-fluorometric (Zimmer-Faust et al. 1988), and electrochemical microprobes (Moore et al. 1989) in aquatic habitats has allowed measurement of the rapid concentration fluctuations characteristic of turbulent plumes at biologically relevant temporal and spatial scales. It is now widely recognized that turbulent chemical plumes consist of discrete propagating packets or filaments separated by non-odor-laden fluid (Murlis and Jones 1981; Moore and Atema 1991; Zimmer-Faust et al. 1988, 1995).

At present, we do not have the means to make predictive hypotheses concerning the distribution of odor filaments in turbulent plumes, nor is it possible to present a comprehensive theory of olfactory-mediated search based on the physical dynamics of a particular habitat. However, we may be able to summarize the statistical properties of dispersing plumes across space and time. If such summaries prove consistent through a range of flow conditions, it may be possible, using only a few physical measurements, to predict odor plume characteristics and to generate hypotheses concerning subsequent animal responses. This capability would provide a major experimental and theoretical advantage over the current necessity of measuring detailed odor plume characteristics in situ for every case of interest.

The statistical tools for describing mean and variance measurements for plume concentration fluctuations have been developed by atmospheric researchers driven mostly by pollution and chemical warfare concerns (Hanna and Insley 1989; Mylne and Mason 1991; Yee et al. 1993*b*). These tools, based predominantly on spectral properties of turbulent plumes and conditional sampling of concentration time series, provide a direct link between the fluid environment and the distributions of chemical stimuli. For example, Mylne (1992) demonstrated that a general description of plume morphology and large scale mixing phenomena such as meandering can be drawn from turbulence measurements in the fluid environment. In addition, Yee et al. (1993*b*) were able to use a single probability density function to describe concentration fluctuations at all points in a turbulent plume. Until now, these techniques have not been applied to the investigation of odor-plume-related behaviors of aquatic organisms.

Alternatively, odor plumes can be described by the distribution of the properties of individual odor filaments. Previous work seeking to couple odor plume measurements with sensory physiology has suggested that characteristics of individual odor filaments in a plume are critical to animal navigation. Under some laboratory conditions, properties of odor packets (such as the steepness of the concentration gradient at the edge of an odor packet) have been shown to vary consistently with distance from the odor source (Moore and Atema 1988, 1991; Zimmer-Faust et al. 1988; but *see* Moore et al. 1994; Atema 1996). As a result, some of these properties have been suggested to provide navigational information to organisms (Moore and Atema 1988, 1991; Zimmer-Faust et al. 1988). However, there is very little known about how such information is distributed or perceived in field environments (but *see* Zimmer-Faust et al. 1988, 1995; Atema et al. 1991).

We examined the dispersal of odor plumes in estuarine tidal channel flows using the two approaches described above. Previous field studies have shown that predators commonly use plumes similar to those studied here to forage in these tidal channel habitats (Zimmer-Faust et al. 1995). In addition, the combination of unidirectional tidal flow, flat bottoms, and steep banks provides a natural, experimentally tractable physical environment for the study of odor dispersal. We present analyses of the hydrodynamic conditions acting to disperse a turbulent plume, the time-averaged concentration profile, the distribution of instantaneous odor-packet properties (sensu Murlis and Jones 1981; Moore and Atema 1988), and the distribution of conditional statistics and the conditional probability density function (sensu Yee et al. 1993*b*). We provide a physical description of plume dispersal and the potential consequences for biological systems.

Methods and statistical analysis

We characterized odor plumes in the field by measuring time-averaged and instantaneous concentration distributions in plumes of conservative tracers and the flow conditions dispersing the plumes. We collected three data sets concurrently for each plume characterization: hydrodynamic measurements of downstream and vertical velocity at 10 Hz; concentration measurements of electrochemical tracer at 10 Hz; and 1-min time-averaged fluorometric concentration measurements. In total, we successfully characterized six plumes in this manner (Fig. 1). From these six trials, a total of 61 hydrodynamic and electrochemical data records and 168 fluorometric samples were collected.

Field site and hydrodynamic characterization—We performed these experiments in tidal channels at Oyster Landing in the North Inlet Estuary at the Belle W. Baruch Marine Field Lab, Georgetown, South Carolina (32°20′N, 79°15′W) during spring and summer 1994. These tidal channels have

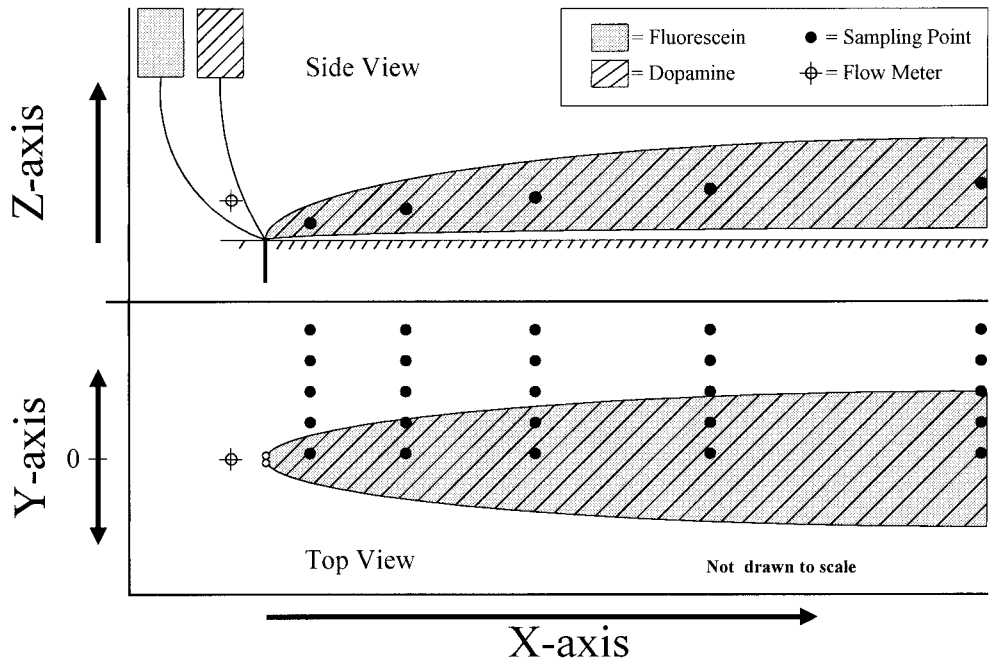

Fig. 1. Schematic view of the field site showing coordinate frame of reference and sampling scheme. The number and spatial arrangement of sampling points differed from trial to trial, although this overall sampling pattern was adhered to. For time-averaged concentration profiles, all cross-stream samples at a given distance from the plume source were collected simultaneously. Individual electrochemical samples were collected serially. This figure is not drawn to scale.

sandy flat bottoms, and water flow is tidally driven and unidirectional for several hours on flood and ebb tides.

Odor plumes are transported by the ambient turbulent flow regime. We measured downstream and vertical components of velocity at 10 Hz with a 1-cm-diameter electromagnetic flow sensor (Marsh-McBirney model 523, 0.1-s time constant) and data logger (Campbell CR10). Each data record consisted of 256 points (25.6 s). The flow sensor was positioned 5 cm above the creek bottom and approximately 10–30 cm upstream from the plume source. Hydrodynamic measurements were synchronized with electrochemical measurements made throughout the plume with the IVEC-10 system. Thus, flow and electrochemical data are synchronized in time but not coincident in space. We assumed that flow conditions were homogeneous within the sampling area, a reasonable assumption given the distance from bends in the creek and the relatively flat sandy bottom of the tidal channel. Obvious large roughness elements (e.g., shells, rocks) were removed prior to plume characterization; however, ripples and mounds were left unaltered. Previous work in this tidal channel showed that roughness heights range from 0.2 cm to 2.2 cm, and analysis of roughness Reynolds numbers (Re_*) showed that boundary layer conditions were transitional or fully rough turbulent for a majority of the tidal cycle (Finelli 1997). Water depth was measured periodically throughout the sampling period. We were restricted to working in the hours surrounding slack low tide because placement of sensors required visual contact with the plume at all times. This results in a somewhat restricted range of depth and flow speed conditions (Table 1). Nevertheless, blue crabs and other organisms actively forage throughout the range of conditions measured here.

Table 1. Summary of flow conditions at the field site during the six plume characterization experiments. Values were used to parameterize the Gaussian model of time-averaged concentration distribution.

Trial	U (cm s^{-1})	U_* (cm s^{-1})	Water depth (cm)
1	3.8	0.17	20
2	3.8	0.20	40
3	6.6	0.20	14
4	7.7	0.19	12
5	9.4	0.24	20
6	35.7	0.92	8

The dispersal of odor plumes in turbulent flows is a function of advection and turbulent diffusion in the water column. We measured advection as the mean downstream velocity (U) and boundary layer turbulence using the friction velocity (U_*, a measure of shear stress at the bed). Using the eddy correlation method, U_* is related to the covariance between the horizontal and vertical components of velocity according to the relation: $U_* = \sqrt{\text{cov}(u' \cdot w')}$, where u' and w' are the deviations from the mean streamwise and vertical components of velocity, respectively (Woodward and Sheehy 1983). Time series of flow measurements were deconvolved before being analyzed statistically. An estimate of mean downstream flow speed (U) and friction velocity (U_*) was calculated for each 25.6-s data record, and a grand mean per trial was determined.

Spectral analysis of flow data—Plume meandering is characterized by sinuous oscillations in the position of the plume as a whole. Such oscillations affect the gross development of the plume and might have bearing on animal navigation. We used spectral analysis to estimate eddy length scales associated with plume meandering by identifying the lower bound of the inertial subrange of the velocity power spectra. Fast Fourier transform (FFT) analysis was used to quantify the spectral characteristics of the velocity time series. Because each velocity time series consists of 256 points (25.6 s) measured at 10 Hz, the FFT produces output in 128 frequency bands ranging from 1/25.6 to 5 Hz, a range that should encompass a majority of biologically relevant data. To reduce artifact introduced by the FFT, flow data were adjusted by subtracting the mean velocity for the data record, dividing by the standard deviation (SAS Institute 1984; Szigaly et al. 1996), and passing the data through a 256-point triangular Bartlett window (maximum value = 1.0) (Jenkins and Watts 1968; Press et al. 1992). Because of signal aliasing, values from frequencies above 3.3 Hz were discarded. Three criteria were used to identify the inertial subrange: the slope of the power spectra, the cospectral density of horizontal and vertical velocity, and the ratio of the spectral density of vertical velocity to spectral density of horizontal velocity.

Simulated odor plumes—For each plume characterization, we created a single highly visible plume of fluorescent dye and electrochemical tracer using a gravity feed drip system (similar to medical intravenous units). We used two tracer solutions: (1) a fluorometric/visual tracer consisting of a 1 g liter^{-1} sodium fluorescein salt (Sigma Chemical) used in creating time-averaged concentration profiles and (2) an electrochemical tracer consisting of a mixture of 2 mM dopamine (3-hydroxytyramine, Sigma Chemical) and 20 mM ascorbic acid (Sigma Chemical) used to measure instantaneous concentration distributions. Tracer solutions were made using artificial seawater (Forty Fathoms) mixed to ambient salinity immediately prior to use. Tracer solutions were released from separate bottles (Toptainer, Ross Industries) through adjoining tubes (Intramedic 7431, 1.1 mm inside diameter). Separate containers and drip tubes were used to avoid precipitation of the fluorescein salt in the presence of the ascorbic acid solution. Outlet tube ends were attached to a stainless steel spike pushed into the sediment. The resulting plume emanated from an essentially single source, 3 × 1.5 mm, positioned at the sediment surface (≤5 mm above the surface) such that inlet flow was nearly parallel to mainstream tidal flow. Input flow rate was set to 6 ml min^{-1} using a thumb roller attached to the tubing, resulting in an inlet velocity of ≈10 cm s^{-1} ($\mathrm{Re}_{\mathrm{jet}} \approx 300$). At this inlet velocity, input flow rate was nearly isokinetic with mainstream flow; thus, the plume was primarily dispersed by ambient turbulent motion rather than its own momentum. This approach stands in contrast to that described by Atema (1996), where plumes were characterized by a strong near-field jet region. In addition, all plume measurements were made at downstream distances >30 times the inlet diameter, placing most measurements outside of the near-field jet region (List 1982).

Time-averaged plume measurements—Time-averaged plume measurements were made using a bank of 12 20-ml syringes drawn simultaneously over a 1-min interval and connected to a sampling ''comb.'' Each syringe was attached to 150 cm of polyethylene tubing (1.1 mm inside diameter). The tubes were spaced along the comb to sample at 0, 2, 4, 6, 8, 10, 15, 20, 25, 30, 35, and 40 cm from the plume midline. Cross-stream profiles were collected sequentially starting at the plume source. We avoided disrupting flow by positioning the comb spine (1.25-cm-diameter dowel) above and downstream from the sampling area. Individual 20-ml samples were kept in glass vials and refrigerated in the dark until fluorometric analysis (Turner model 110). The practical limit of detection of fluorescein for the Turner 110 fluorometer is 10^{-6} g liter^{-1}. All measured values below 10^{-6} g liter^{-1} were discarded.

Time-averaged concentration profiles vs. Gaussian model—Time-averaged concentration profiles for each plume were compared with a Gaussian model modified for application to depth-limited boundary layer conditions. The model takes the form:

$$C_{x,y} = \frac{Q}{\sqrt{2\pi}Uh\sigma_y}\exp\left(\frac{-y^2}{2\sigma_y^2}\right),$$

where $C_{x,y}$ is the concentration at downstream position x and cross-stream position y, Q is the input rate of diffusing solute (=0.0001 g s^{-1} in these experiments), U is the mean downstream velocity, h is the total water depth, and σ_y is a factor related to the rate of cross-stream spread (Pasquill and Smith 1983); $\sigma_y = (\alpha_y U_* x)/U$ where U_* is the friction velocity and α_y is an empirical constant set to 2.2 for this study (Denny 1988). All modeled values $<10^{-6}$ g liter^{-1} were discarded for consistency with measured values.

The measured time-average concentration distribution was compared with the modeled values using a series of regression analyses. We regressed the measured concentration data against predicted values and tested the slope for difference from 1 to determine how well the Gaussian model predicts the time-averaged concentration profile. To determine the rate of change in concentration down the centerline of the plumes, each concentration value was normalized to the maximum predicted or measured concentration ($C_{\max}$) (usually the point closest to the source). This approach places all data on a relative nondimensional scale between 0 and 1. We used nonlinear least-squares regression to fit a curve to both the predicted and the measured concentration profiles (SAS Institute 1984). The regression curves were of the form $C_{x,0} = c_o e^{-\lambda t}$, where $C_{x,0}$ is the concentration at a given location, x, down the midline of the plume, c_o is the initial value of normalized concentration, and λ is the rate of exponential decrease.

Electrochemical plume measurements—High-frequency fluctuations in odor concentration are characteristic of turbulent odor plumes and may provide directional information to a navigating organism. We measured such fluctuations at 10 Hz using a customized In Vivo Electro-Chemistry System and microprobe (IVEC-10, Med-Systems). Using this sys-

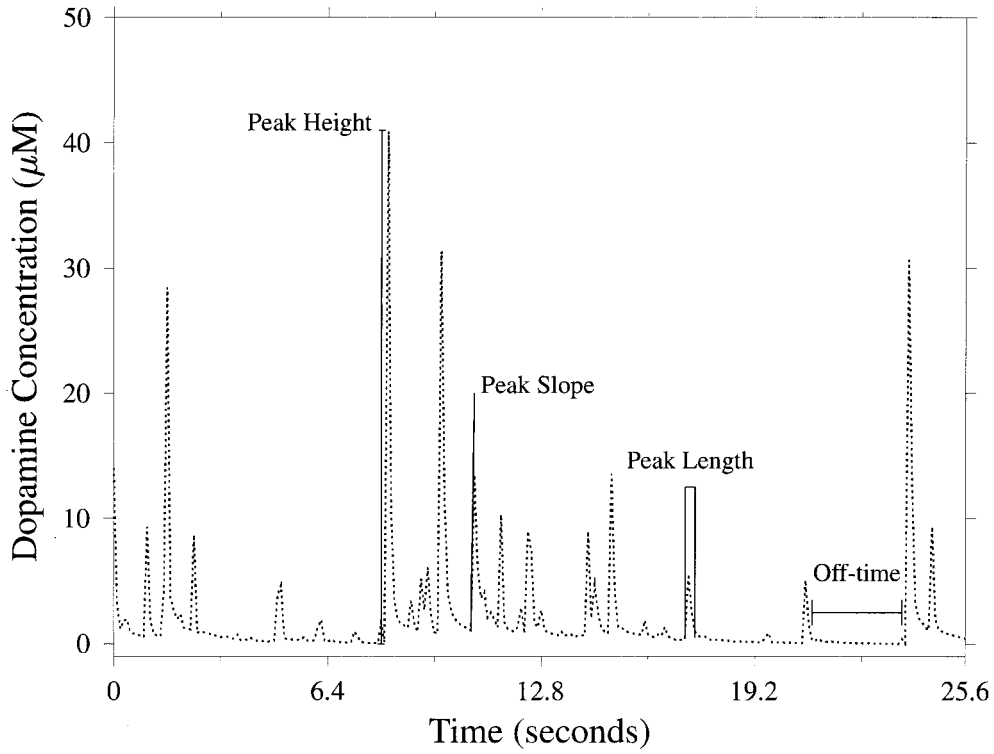

Fig. 2. Representative concentration time series of dopamine as measured at a stationary point by the IVEC-10 electrochemical probe (dashed line). The measurement of the following odor filament characteristics is indicated: peak height, peak length, peak slope, and off-time. Definitions of these quantities follow Murlis and Jones (1981) and Moore and Atema (1988).

tem, tracer concentration is proportional to the electric current induced by the oxidation of dopamine at the surface of a 150-μm triple carbon fiber electrode. We calibrated individual concentration traces and corrected for sensor drift using sensor calibrations made immediately before and after each trial. Data were serially collected from discrete sampling locations within the plume, starting at the plume source and moving cross-stream before moving to the next location downstream. We collected 60–70 s of data at each sampling point within the plume, of which 25.6 s (256 points) were used in statistical analysis. Data segments were chosen arbitrarily, but we avoided the first and last 5–10 s of the data record. Each time series of dopamine concentration was deconvolved prior to statistical analyses.

The odor filaments that produce the high-frequency concentration fluctuations measured by the IVEC-10 system can be described by a number of parameters introduced by Murlis and Jones (1981) and subsequently modified by Moore and Atema (1988). These parameters are the peak height, maximum peak slope, peak length, number of peaks, number of off-time periods, and duration of off-time periods (Fig. 2). A concentration peak begins when the instantaneous concentration rises above the lower limit of instrument detection, 0.1 μM, and ends when concentration dips below this threshold. Off-time is the period between successive peaks. Peaks not separated by an off-time period are considered different if the intervening low point is $<$30% of the preceding peak height. Peak length is the time between the beginning and end of a peak. Maximum peak slope is the maximum rate of change in concentration on the rising side of the concentration peak. Peak height is the maximum concentration of a given peak. Because a given concentration trace has multiple peaks, mean values of these parameters were calculated for each spatial position.

The centerline distributions of odor filament characteristics were analyzed using nonlinear regression techniques (SAS Institute 1984). Centerline profiles of mean concentration, variance, peak slope, and peak height were normalized to the maximum value measured along the centerline of each plume (C_{max}, Var_{max}, $Height_{max}$, and $Slope_{max}$), and the normalized values were fitted with a nonlinear least-squares regression. Because we were interested in the relative rates of decay in measured filament characteristics with distance from the plume source, the normalization and nondimensionalization scheme allowed us to compare the centerline profiles of all nondimensionalized parameters, including the time-averaged concentration.

Conditional statistics and exceedance properties—Conditional statistics, in which all samples with no detectable tracer are removed, have been widely used in the interpretation of atmospheric plume data. The spiky nature of the instantaneous plume results from incomplete mixing of clean water into the plume during initial plume formation and from entrainment of clean water by turbulent eddies at the plume's edge (List 1982; Mylne 1992). Conditional sampling of the

instantaneous plume in our case entailed the removal of all samples below the threshold for detection (0.1 μM). Once the concentration time series was conditionally sampled, conditional mean concentration and conditional variance were calculated. The local signal intermittency, which is defined as the proportion of time that the concentration is above threshold values, was also calculated from the conditionally sampled time series. Nonlinear least-squares regressions were fitted (as described above) to the centerline profiles of the normalized conditional mean, conditional variance, and intermittency.

It is often convenient to summarize the temporal distribution of instantaneous odor concentration as the probability that instantaneous odor concentration will exceed a given proportion of the local mean concentration. To do so, the raw concentration time series was sampled conditionally, and the local mean conditional concentration was calculated. Each concentration sample in the conditional time series was then normalized to the local conditional mean for that time series. Probability density functions (PDFs) were then generated from the calculated probability of encountering odor of a given normalized concentration; 61 PDFs were estimated. The mean probability distribution was calculated for normalized concentrations from all 61 data records and plotted with the standard deviation.

Deconvolution of flow and IVEC data—Data collected by the IVEC electrochemistry system and the Marsh–McBirney flow probe are subject to artifact resulting from signal ''memory,'' which results in an exponential rather than instantaneous change of the signal after a step change in the data (sensor impulse response). In other words, after application or removal of the stimulation of the sensor, the output signal does not track the true signal immediately. The sensor signal response is exponential, taking the form $c_t = c_o e^{-\omega t}$, where c_t is the measured quantity (dopamine concentration or flow velocity) at time t, c_o is the initial true signal strength, ω is the time constant (decay constant), and t is time (Horowitz and Hill 1989). To remove this artifact, each data record was deconvolved using Fourier transform methods prior to any statistical analyses. Deconvolution is simply the division of the Fourier transform of the data record by the Fourier transform of the appropriate exponential function (impulse response function of the sensor) (Jenkins and Watts 1968; Press et al. 1992).

In the case of the Marsh–McBirney flow probe, the exact form of the response function is known. By instrument design the time constant $\omega = 1.0$ (ω = sensor time constant/sample interval = 0.1 s/0.1 s). Setting the area under the curve to 1.0 and integrating results in a final form of the decay function used in deconvolution of flow data of $c_t = 1.0e^{-1.0t}$.

The time constant of signal decrease is unknown for the IVEC system. To estimate this coefficient, individual signal spikes (near-instantaneous tracer arrival and removal) were isolated from various traces, and the exponential constant was fitted using nonlinear least squares regression. Twenty-five such regressions were used to calculate a mean time constant, ω, of 0.454 ($\pm$0.104 SE). Setting the area under the curve to 1.0 and integrating the function results in an impulse response function used in deconvolution of electrochemical traces of $c_t = 0.454e^{-0.454t}$.

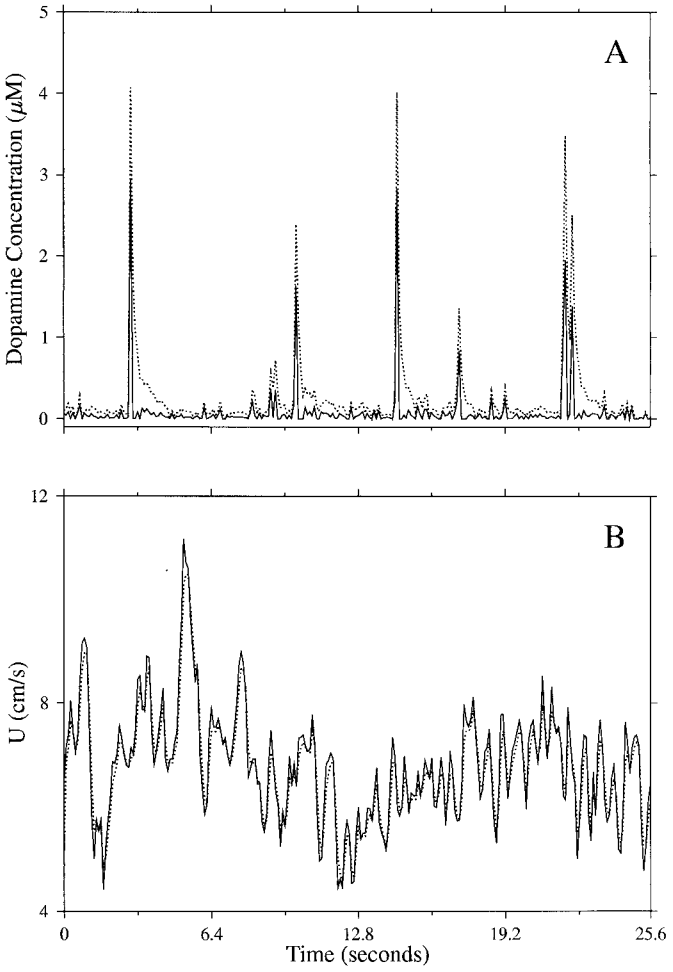

Fig. 3. Representative dopamine concentration (A) and downstream velocity (B) time series showing the effect of deconvolution. Solid lines represent the time series after deconvolution; dashed lines represent the raw time series. The effect of deconvolution is much more pronounced on the dopamine concentration measurements, effectively separating individual odor spikes that may otherwise appear as a single event.

The effect of the deconvolution on flow records is minimal (Fig. 3B) compared with that on the electrochemistry data (Fig. 3A). The main effect on electrochemical measurements is to further separate adjacent concentration spikes that might otherwise appear to be part of the same event, as can be seen for the two large peaks at the far right of the trace in Fig. 3A.

Spectral properties of turbulent flow—A simple conceptual model of turbulent flows can be based on the spectral properties of velocity fluctuations (Kolmogorov 1941; Kaimal and Finnigan 1994; Szigaly et al. 1996). The lowest frequencies of the velocity power spectrum represent the largest, most energetic eddies. As these large eddies are sheared, kinetic energy is transferred to progressively smaller eddies. At intermediate scales, an eddy cascade exists in

which turbulent kinetic energy is neither created nor destroyed but simply transferred to smaller scales of motion. The highest frequency smallest eddies act to transform the kinetic energy to heat through viscous dissipation.

The lowest frequency bands of the inertial cascade determine the scales over which a plume will appear to meander, a potential problem for navigating animals. Kaimal and Finnigan (1994) described three criteria for the identification of the inertial subrange: (1) a $-5/3$ slope in a log-log plot of power vs. frequency (this is the 5/3 power law first described by Kolmogorov [1941] in which $S(n) \propto n^{-5/3}$, where $S(n)$ is the spectral density at frequency n); (2) the cross-spectrum, a measure of covariance in the frequency domain, of horizontal and vertical velocity within the inertial subrange tends towards zero (this phenomenon results from isotropy of the smallest eddies in a turbulent flow, i.e., they have no preferred directionality); and (3) the ratio of the spectral density of vertical velocity to the spectral density of downstream velocity is approximately 4/3, i.e., $S_w(n)/S_u(n) \approx 1.33$.

To identify the inertial subrange, we applied these three criteria to each of the flow data records. Visual inspection of the output allowed narrowing of the frequency range for analysis to 0.8–3.3 Hz. In this frequency range, there was general agreement between predicted and measured values of the power spectrum slope and cross-spectral densities (Fig. 4). The mean slope measured through the power spectra = -1.64 (vs. -1.67 predicted by theory), and the mean cospectral density = -0.0005 (vs. 0.0 predicted by theory). The third piece of evidence, the ratio $S_w(n)/S_u(n)$, does not agree as well, with a mean value of 0.93 in contrast to the predicted value of 1.33. Constraints on eddy structure due to limited water depth during these experiments are probably responsible for this disparity. In depth-limited situations, spectral energy normally present in the vertical dimension will be transferred to the less-constrained horizontal dimensions, thus decreasing the value of $S_w(n)/S_u(n)$. We conclude that we have correctly identified the lowermost portion of the inertial subrange (the uppermost bound, which is $\gg$10 Hz, could not be resolved). To a first approximation, the length scales that determine plume meandering will be related to motions occurring at approximately 0.8 Hz.

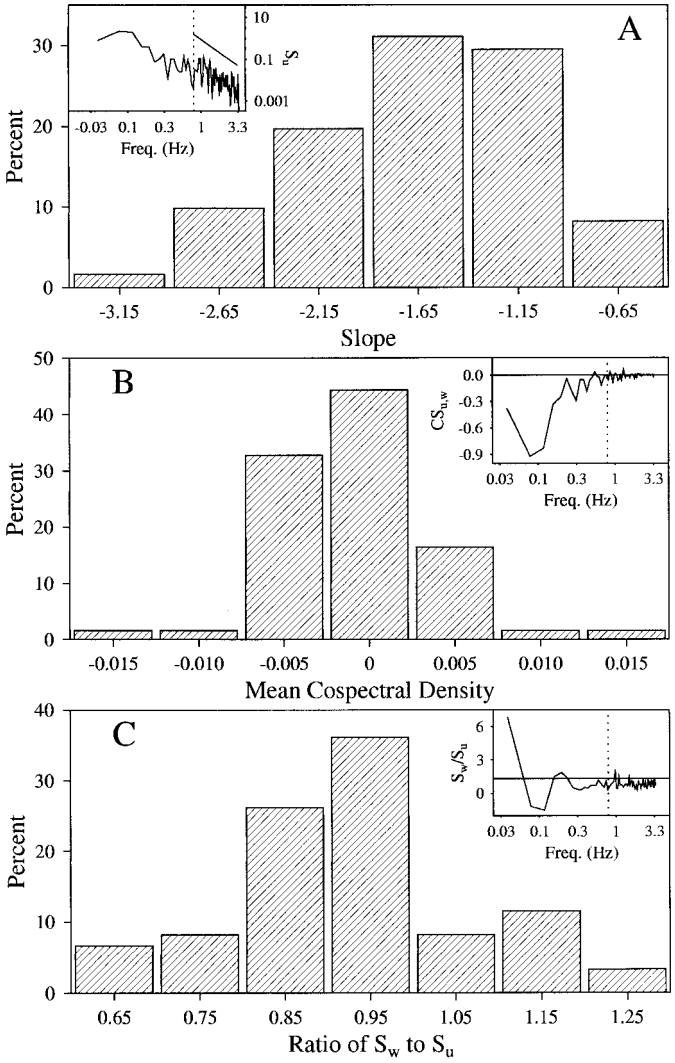

Fig. 4. Summary of spectral properties used to identify the lower bound of the inertial subrange in the velocity power spectrum. (A) Frequency histogram of the slope measured through the power spectra in a frequency range of 0.8–3.3 Hz for all velocity records (n = 61). *Inset:* Typical velocity power spectrum. Dashed line is lower bound for inertial subrange (0.8 Hz); solid line shows $-5/3$ slope. (B) Frequency histogram of mean cospectral density of horizontal and vertical velocity for all velocity records (n = 61). *Inset:* Typical cospectrum. Dashed line is the lower bound of inertial subrange (0.8 Hz); solid line at cospectral density = 0. (C) Frequency histogram of the ratio between the log of spectral density of vertical velocity and the log of the spectral density of downstream velocity for all velocity records (n = 61). *Inset:* Plot of the ratio versus frequency. Dashed line is the lower bound of the inertial subrange; solid line is at ratio = 1.33.

Results

Representative data sets—For each plume characterization, time-averaged concentrations, instantaneous concentration time series, and flow velocity time series were collected. Figure 5 illustrates the raw data collected for trial 5 and shows the spatial variation in instantaneous (multiple time series) and time-averaged (histograms) concentration typical of the observed odor plumes. As would be expected, concentration is highest at the plume source and declines downstream and cross-stream in both the instantaneous and time-averaged concentration measurements. Time series of electrochemical data reveal highly variable temporal distribution of odor packets (concentration spikes). Significantly, meandering of the plume past the sensor can be detected close to the plume source as long periods of high concentration separated by long periods of no odor. Although multiple hydrodynamic data records were collected (one throughout each electrochemical time series), only one data set indicates that flow data were limited to one spatial coordinate. From these, and similar time series for the vertical velocity, estimates of mean advective velocity (U) and mean shear velocity (U_*) were calculated. Here, we present summary data for trial 5 followed by summary statistics from all six trials. Trial 5 was chosen because the flow speed

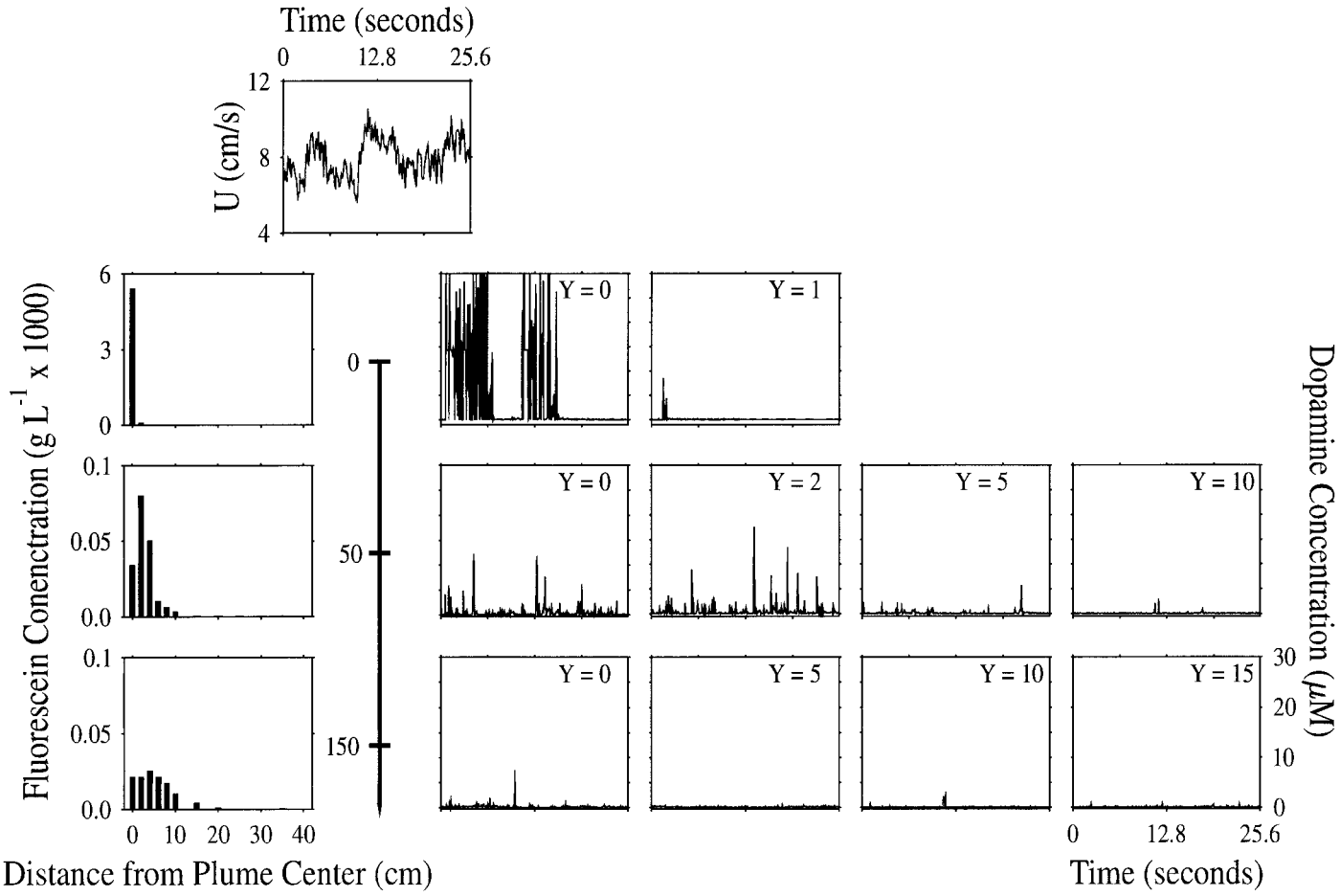

Fig. 5. Composite view of the three data sets collected for trial 5. Distance from the odor source is noted by bold arrow located to the left of center. At top center is a single 25.6-s time series of downstream velocity measured by the electromagnetic flow probe located upstream from the plume source. This time series corresponds in time to only one of the electrochemical data sets. Similar flow data sets correspond to each of the serially collected electrochemical data sets. Histograms to the left of the arrow are time averaged fluorescein concentrations in the downstream and cross-stream dimensions. Note change in concentration scales (*y*-axis) of the histograms with distance from the source. Time-series to the right depict the concentration of dopamine as measured by the IVEC-10 electrochemistry system. Position cross-stream is noted in the upper right corner of each concentration trace.

during this trial is at neither a high or low extreme, and electrochemical measurements were made at 10 spatial locations, thus permitting detailed characterization.

Analysis of flow records—Plume characterizations were completed through the natural range in flow conditions found in this tidal channel. Water depth was between 8 and 40 cm during the six experimental trials (Table 1). Downstream velocity (U) ranged over approximately a factor of 10, whereas U_* ranged over a factor of 5. These values, including water depth, were used to parameterize the Gaussian model of time-averaged concentration. Spectral analysis of the velocity records indicated the presence of the inertial subrange of 0.8–3.3 Hz. Because the electromagnetic flow probe was positioned just upstream from the plume source, eddies shed from the probe can influence the distribution of odorant. Given a diameter of 1 cm, flow speeds ranging from 3.8 to 35.7 cm s^{-1}, and kinematic viscosity of seawater of $\approx$0.01 cm^2 s^{-1}, the Reynolds number of the probe ranged from 380 to 3,570. The corresponding range of Strouhal numbers for this range of Reynolds numbers is 0.18–0.21 (Vogel 1994). These Strouhal numbers indicate that vortices will be shed from the probe at a rate of 0.7–7 Hz, depending on flow speed. We saw no indication in the power spectrum of either the flow data or the electrochemical data of anomalous peaks in the data corresponding to frequencies in this range.

Time-averaged concentration profiles vs. Gaussian model—The form of the measured time-averaged concentration distributions matches that of the Gaussian model for trial 5 (Fig. 6). The distribution shown in Fig. 6A is typical of all six trials, exhibiting exponential decrease downstream and a bell-shaped cross-stream profile with maximum concentration at the centerline of the plume. Figure 6B shows the corresponding model predictions. A log-log regression of measured vs. predicted concentration produces a slope not significantly different from 1 for all data (Fig. 7: slope =

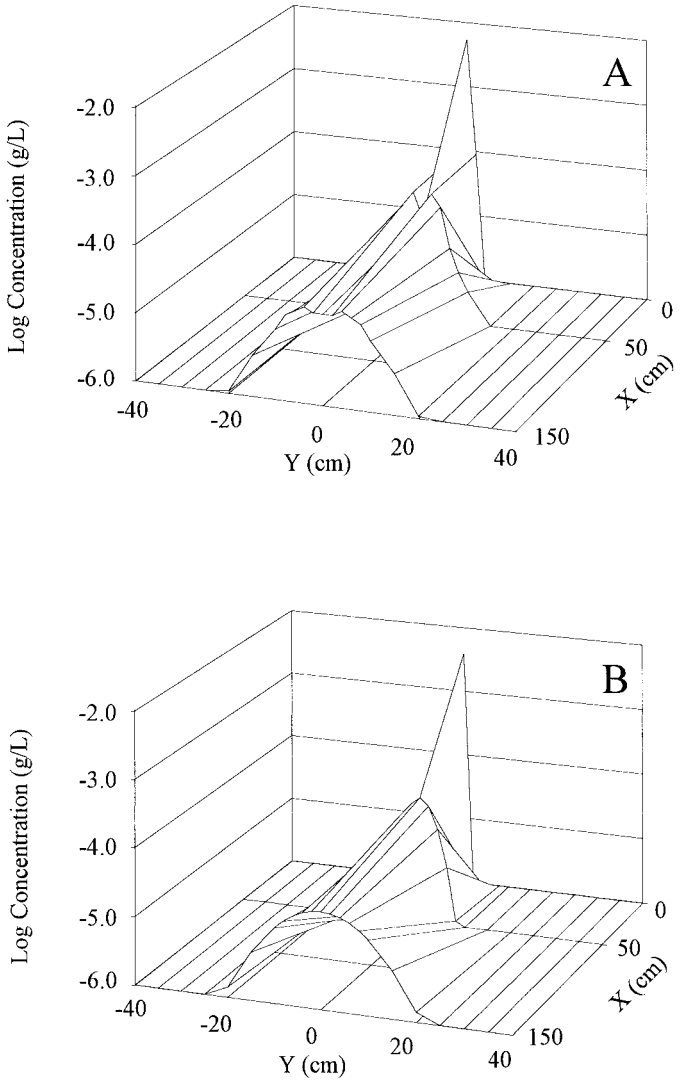

Fig. 6. Distribution of the time averaged fluorescein concentration in the downstream (X) and cross-stream (Y) dimensions for trial 5. (A) Measured concentrations of fluorescein dye. (B) Concentration predicted using the Gaussian model described in the text. For both plots, data are reflected across the *y*-axis to depict an entire plume, although measurements were only made in the positive Y direction.

0.89, $P = 0.24$). The same result is obtained analyzing each plume individually (experimentwise $P > 0.05$ for Bonferroni-adjusted comparisonwise $\alpha = 0.05/6$). Centerline profiles (Fig. 8) of measured (A) and modeled (B) time-averaged concentration are very similar and decrease exponentially ($P < 0.001$ in both cases). There is some discrepancy between the modeled and measured values for any given trial; however, the overall pattern is robust.

Analysis of high frequency concentration measurements—Distributions of mean concentration, concentration variance, mean peak slope, and mean peak height (Fig. 9A–D) are remarkably similar and bear a qualitative resemblance to the time-averaged concentration profiles (Fig. 6A). Centerline profiles of normalized concentration, normalized concentration variance, normalized peak slope, and normalized peak height decline exponentially with distance downstream at similar rates (Fig. 10, $P < 0.001$ in all cases).

Conditional statistics and exceedance probabilities—The distributions of conditionally sampled mean and variance statistics for trial 5 show a high degree of similarity (Fig. 11A,B) and qualitative resemblance to the distribution of time-averaged concentration (Fig. 6A). Centerline profiles of conditional concentration and conditional concentration variance decrease exponentially with distance from the plume source (Fig. 12, $P < 0.001$ in all cases). Because of conditional sampling (the removal of samples with concentration below detectable levels), the rate of decay is less than that observed for the time-averaged concentration (Fig. 8) or odor packet properties (Fig. 10). In general, the intermittency decreases with increasing distance from the plume center and increasing distance from the plume source (Figs. 11C, 12). However, in three trials intermittency values measured close to the plume source were relatively low (Fig. 12), which appears to be a function of the plume meandering close to the plume source.

It is convenient to express the concentration distribution in terms of the exceedance PDF. This PDF indicates the probability that the odor concentration at a given time and location exceeds some multiple of the local mean concentration for that time series. The distribution of exceedance probability is similar in all plumes and all positions within the plumes. There is a high probability, approaching unity, that the odor concentration at a given time and location is >1% of the mean concentration (Fig. 13). In contrast, there is approximately a 10% probability that the concentration at a given time equals or exceeds the conditional mean and a 1% probability that the concentration exceeds 10 times the conditional mean (Fig. 13).

Discussion

In this field study, we used two approaches to quantify turbulent odor plume dispersal in natural marine habitats. The first relies on statistical methods developed by atmospheric researchers and is based on the spectral properties of the turbulent plume and the conditional sampling of the concentration time series. The second approach focuses on the time-averaged and instantaneous distributions of odor concentration. Specifically, we measured the time-averaged concentration, characteristics of individual odor packets (e.g., peak slope), and conditional statistics in plumes under a variety of natural flow conditions. Each of these distributions is characterized by exponential decrease down the centerline of the plume and a bell-shaped distribution cross-stream (Figs. 6–12), and all show a remarkable degree of similarity to each other. In addition, these empirical distributions seem to be qualitatively and, in some cases, quantitatively similar to model results based on the Gaussian statistical distribution. Even more striking is the degree of overlap in the exceedance PDFs from all locations within and among plumes (Fig. 13).

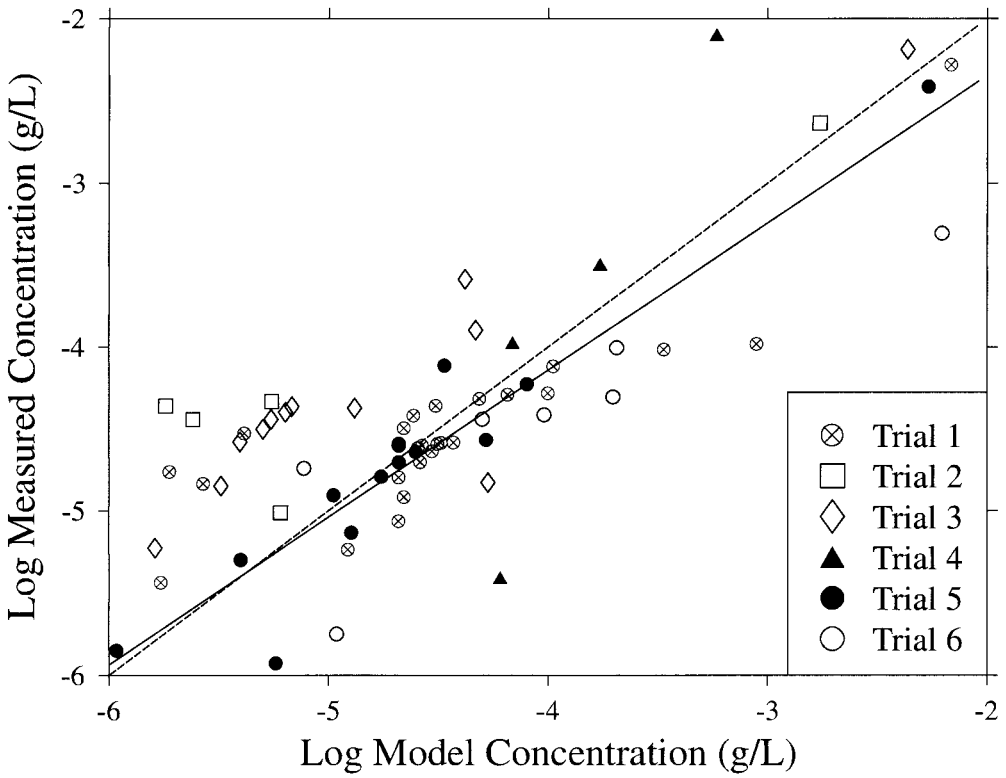

Fig. 7. Log-log plot of measured time-averaged fluorescein concentration vs. time-averaged concentration predicted from the Gaussian model for all trials. Solid line indicates regression line with slope = 0.89 (r^2 = 0.6294; H_o: slope = 0, P = 0.0001, F = 110, df = 1,65); H_o: slope = 1, P = 0.2375, F = 1.4, df = 1,65). Dashed line indicates a line with a slope of 1.

Turbulent eddy size and plume meandering—Mylne (1992) presented a conceptual model of the formation of a turbulent plume based on its width relative to the eddy length scales present in the turbulent flow. According to this model, when the plume is very narrow as compared with dominant eddy length scales, the entire plume will meander (traverse laterally). As the plume width approaches the dominant eddy length scales, non-odor-laden fluid is mixed into the interior of the plume from the edges. If the plume width exceeds these dominant length scales, vigorous mixing occurs in the interior of the plume.

We estimated the eddy length scales that cause plume meandering by identifying the inertial subrange of eddy sizes in the frequency-power spectra of flow velocity time series. The frequency band at the beginning of the inertial subrange is typically the most energetic and thus represents the dominant eddy length scale responsible for large-scale meandering (Hanna and Insley 1989; Yee et al. 1993*a*). This length scale can be estimated by U/n, where n is the dominant energy-containing frequency. Taking the range of velocities in this study (3.8–35.7 cm s^{-1}) and a dominant frequency of 0.8 Hz, eddy length scales responsible for plume meandering range from 5 to 45 cm. Given depth and channel size constraints present during these experiments, this range of eddy length scales is a reasonable first approximation but should not be considered any more than a rough estimate of eddy structure.

Under the conceptual model presented by Mylne (1992), plumes in these tidal channels should exhibit very little meandering after the first 25–50 cm. For example, the dominant eddy length scale during trial 5 (U = 9.4 cm s^{-1}) was on the order of 12 cm. This plume reached a width of 12 cm well within the first 50 cm (Figs. 5, 6). Meandering was evident close to the source during this trial (Fig. 5, X = 1, Y = 0) as the entire plume moved back and forth over the sensor, causing alternating periods of high concentration followed by zero concentration. This pattern was not evident further downstream. In times of slowest flow, the width of the plume rapidly exceeded the dominant eddy length scales, and no meandering was observed. In the fastest flow, where plumes tend to be straight and narrow, meandering was prevented by limited water depth and the dominance of advection.

Meandering was rarely evident under our field conditions, thus it should not have influenced animal performance in these habitats. For example, blue crabs respond to the presence of odor by moving in an upcurrent direction using rheotaxis, and when the odor signal is lost (because of dilution, plume meandering, or walking out of a plume), the crabs move in the cross-stream direction or hesitate until the plume is recontacted (Weissburg and Zimmer-Faust 1993, 1994; Zimmer-Faust et al. 1995). Mixing lengths estimated in this study are on the order of 5–45 cm, causing small meanders only very near the odor source and resulting in relatively straight and narrow plumes that crabs can follow directly to the source, with few turns or periods of hesitation (Zimmer-

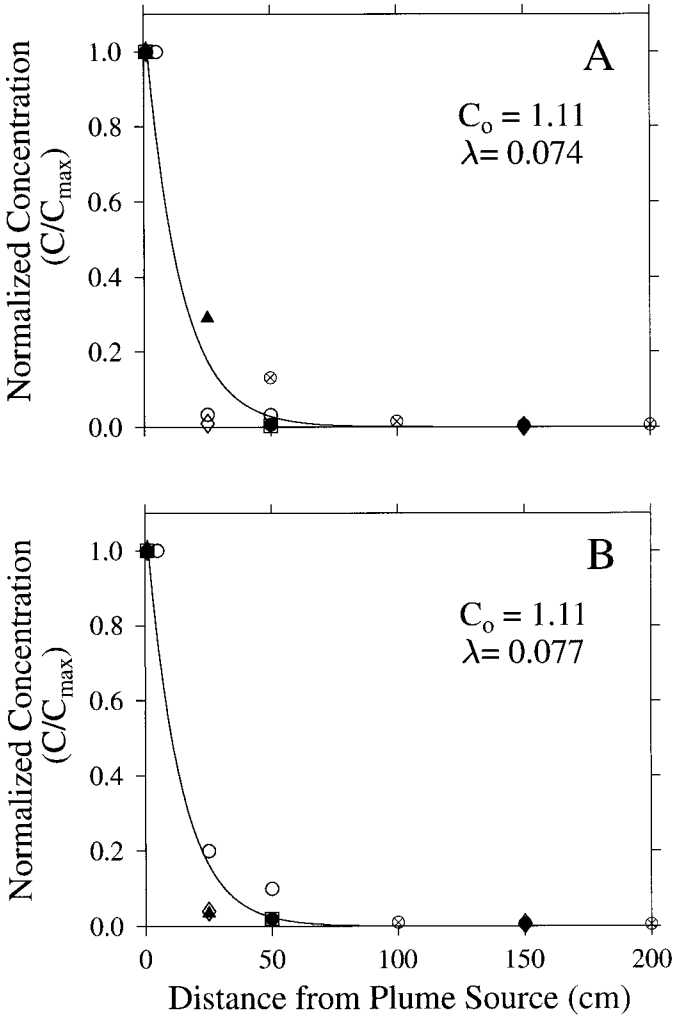

Fig. 8. Centerline profiles of time-averaged concentration normalized by the maximum measured concentration in the centerline, usually point closest to the source, for all trials. (A) Measured profiles of time-averaged fluorescein concentration. (B) Profiles predicted by Gaussian model. C_o and λ values indicate regression values used in fitting exponential model to data; solid line indicates least squares regression line. (A) $r^2 = 0.2236$, $P < 0.001$. (B) $r^2 = 0.2361$, $P < 0.001$. Symbol key as in Fig. 7.

Faust et al. 1995; Finelli 1997). However, in less physically constrained habitats, plume meandering can interfere with olfactory-mediated search by removing the olfactory signal from the organism for long intervals of time. For example, dominant length scales measured in terrestrial habitats used by moths during pheromone communication are on the order of 1–10 m (Mylne 1992; Davidson et al. 1995). Meandering in these conditions can exist more than 100 m downwind from the plume source (Mylne and Mason 1991). Thus, the plume may meander away from an orienting moth by many meters, a substantial distance for an animal measuring only a few centimeters in length. This meandering may cause the moth to engage in relatively frequent bouts of counterturning flight while trying to recontact the plume (Murlis et al. 1992; Kuenen and Carde 1994). Of course other variables will contribute to the overall direction of odor-mediated search (e.g., flow speed and direction, rates of odor dilution, odor filament structure); however, quantities such as the extent of plume meandering that describe the gross form of the odor plume and can be estimated from relatively simple physical measurements should not be discounted in an analysis of odor-mediated search behavior. Unfortunately, flume and wind tunnel studies (and even simplified field studies such as this) often minimize the impact of larger scale plume phenomena.

Intermittency and conditional statistics—Within a turbulent plume, meandering and incomplete mixing of clean water into the plume center result in a patchy distribution of odor-laden water interspersed with clean water. Time periods of zero odor concentration (off-time) play a fundamental role in determining the overall distribution of olfactory information. A unified measure of off-time periods is the intermittency (Fig. 11C), defined as the proportion of time the concentration exceeds zero (Yee 1990; Mylne and Mason 1991). The intermittency of a turbulent plume represents a potentially powerful navigational cue to a searching organism, especially when combined with ancillary cues such as flow speed and direction. For example, as an organism moves toward the center of the plume or closer to the odor source, the proportion of time odor is detected above background (intermittency) increases or remains constant (Figs. 11C, 12C). Blue crabs respond to odor plume in a binary (presence/absence) manner by moving upstream when odor is present and moving cross-stream (or hesitating) when odor is absent (Weissburg and Zimmer-Faust 1993, 1994; Zimmer-Faust et al. 1995; Finelli 1997). Such a locomotory pattern is consistent with an organism that responds to intermittency thresholds. For example, blue crabs may move upstream when intermittency is high and may move cross-stream (or hesitate) when intermittency is low (Weissburg and Zimmer-Faust 1994; Zimmer-Faust et al. 1995). Such a sampling scheme would require that the animal detect only the presence of odor concentrations above some threshold level sequentially through time. Further study of animal behavior in relation to plume intermittency should elucidate what role this parameter plays in odor-mediated orientation.

Conditional sampling of the turbulent odor plume allows the distribution of instantaneous odor concentration at any point in the plume to be described by a single exceedance PDF (Fig. 13). The probability distribution presented here is qualitatively and quantitatively similar to PDFs for atmospheric plumes presented by Yee et al. (1993*b*). This powerful analysis collapses all of the concentration fluctuation data into a single curve from which stochastic variation in concentration can be incorporated into future models of plume structure. For example, the conditional mean concentration can be predicted using a form of the Gaussian distribution, and instantaneous concentration at a given time step can be stochastically varied using the exceedance PDF. The incorporation of intermittency and hydrodynamic information into models of conditional concentration distributions should yield powerful plume models that can be used for hypothesis testing as our knowledge of olfactory physiology increases.

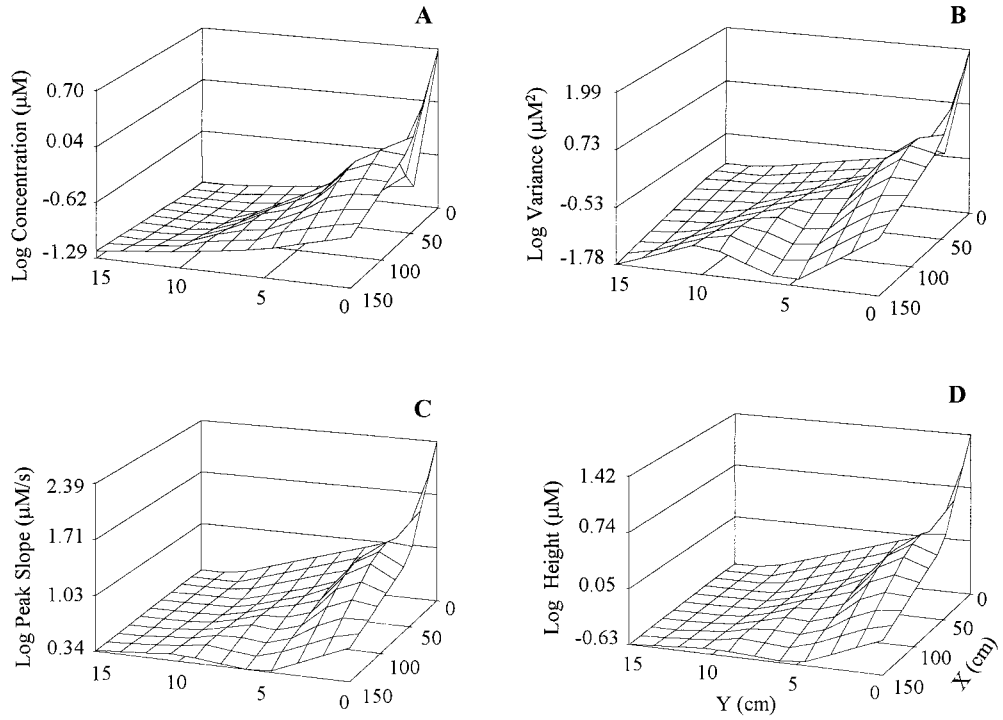

Fig. 9. Downstream and cross-stream distributions of mean odor-packet properties measured from dopamine concentration time series from trial 5. Data are not reflected across the *y*-axis.

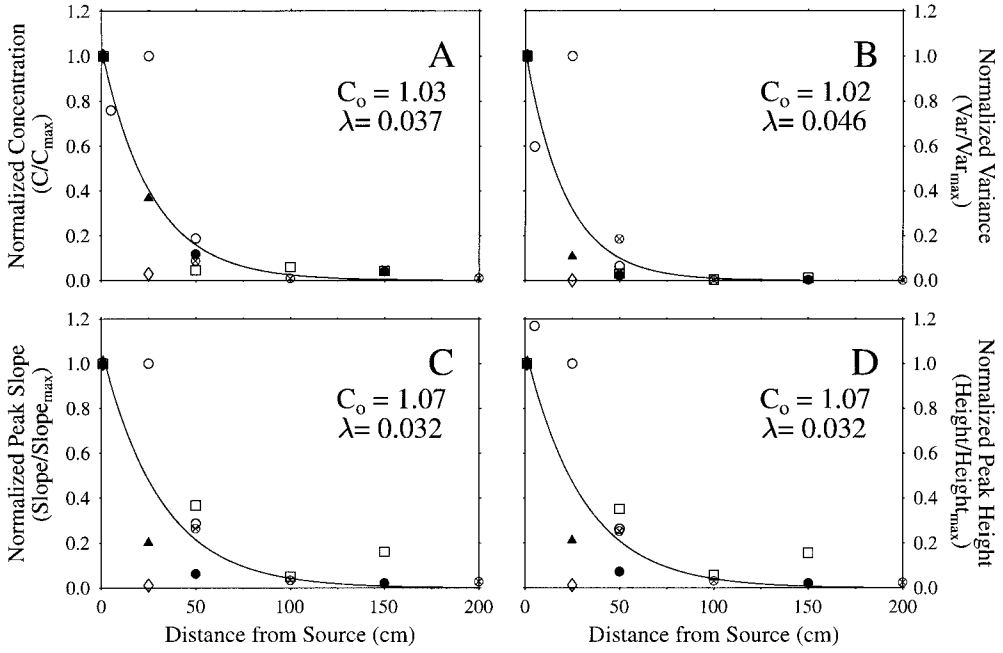

Fig. 10. Centerline profiles of odor packet properties measured from the dopamine time series from all trials. All values normalized to the maximum measured value for the centerline profile. C_o and λ values indicate regression coefficients used to fit exponential model to data; solid line depicts least squares regression. (A) $r^2 = 0.1828$, $P < 0.001$. (B) $r^2 = 0.1722$, $P < 0.001$. (C) $r^2 = 0.1940$, $P < 0.001$. (D) $r^2 = 0.1940$, $P < 0.001$. Symbol key as in Fig. 7.

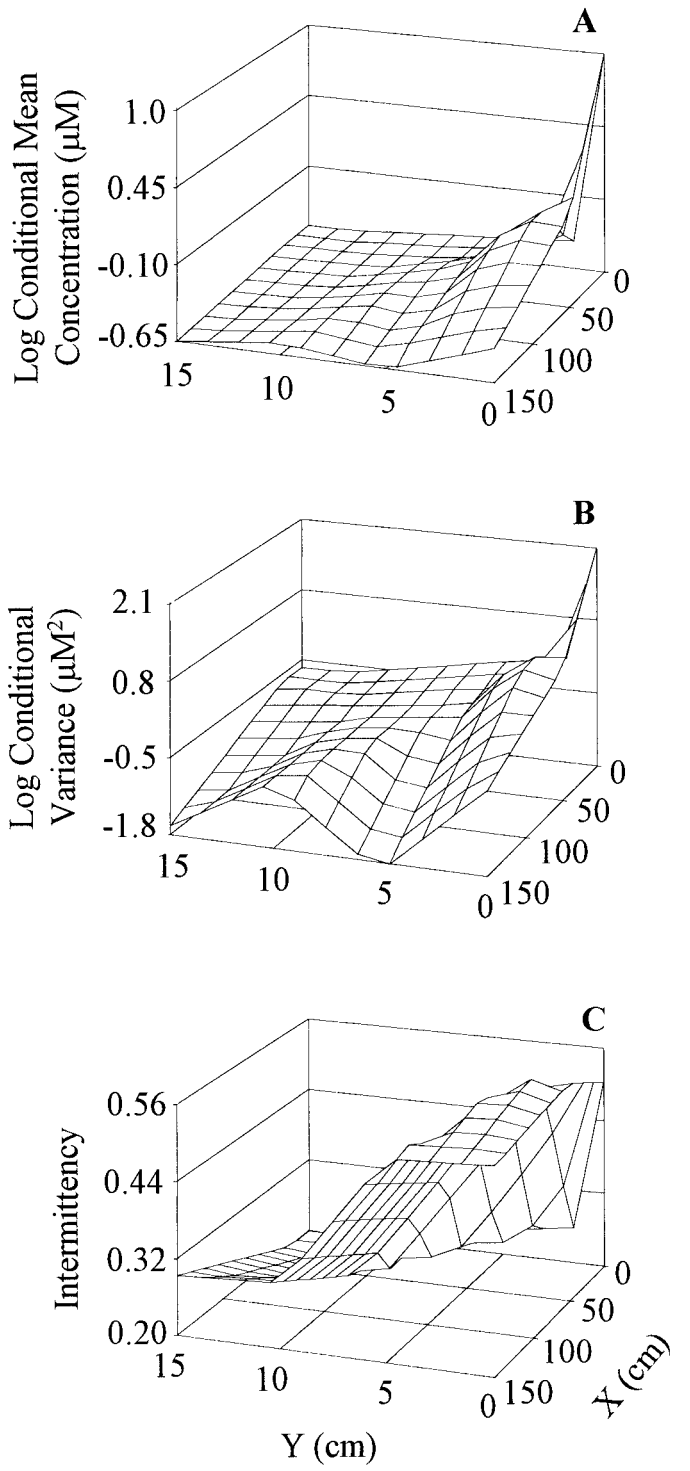

Fig. 11. Distribution of conditional mean concentration (A), conditional variance (B), and intermittency (C) in the downstream and cross-stream directions from trial 5.

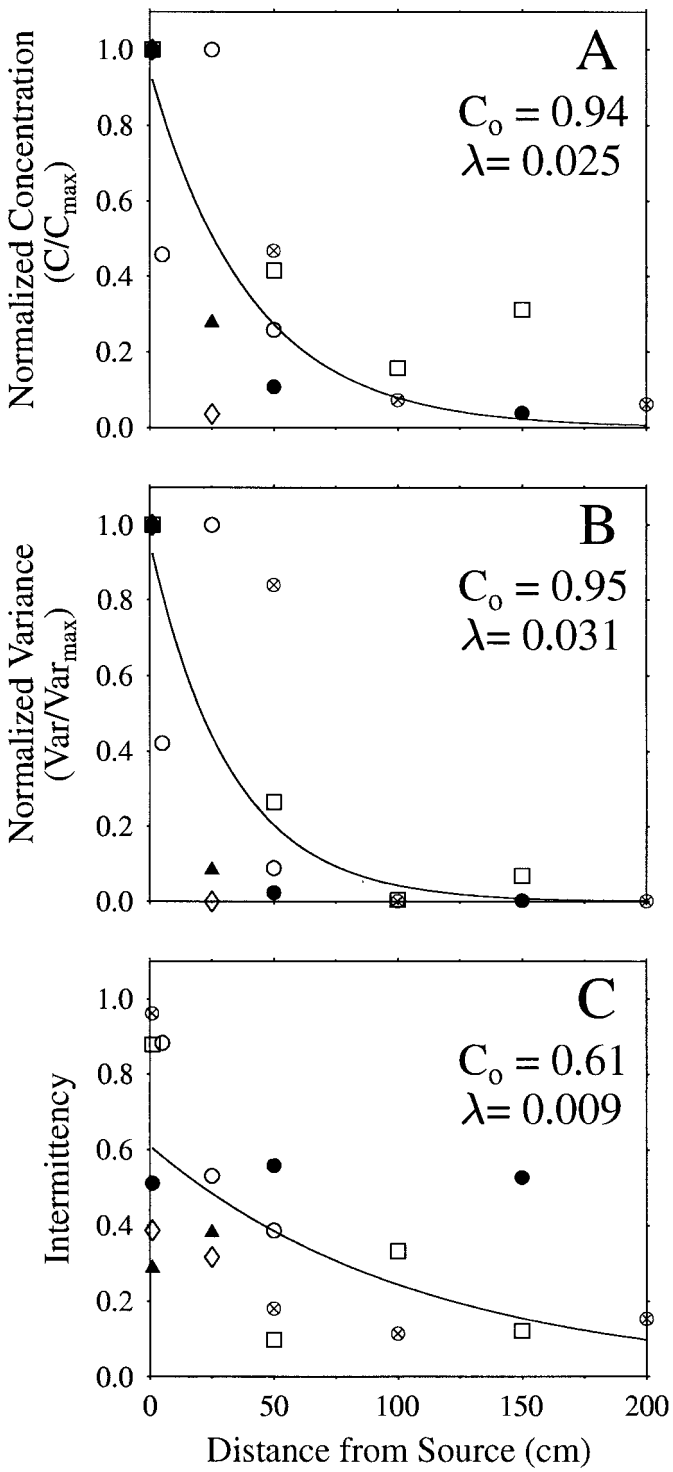

Fig. 12. Centerline profiles of conditional mean, conditional variance, and intermittency for all trials. C_o and λ values are regression coefficients used to fit exponential model to the data. Solid line indicates least squares regression line. (A) $r^2 = 0.2232$, $P < 0.001$. (B) $r^2 = 0.1985$, $P < 0.001$. (C) $r^2 = 0.3093$, $P < 0.001$. Symbol key as in Fig. 7.

Time-averaged concentration and odor filament properties—Time-averaged concentration distributions are easily measured and match predictions of a standard Gaussian model (Figs. 6–8). Significantly, the time scales needed to generate such profiles are much longer than those associated

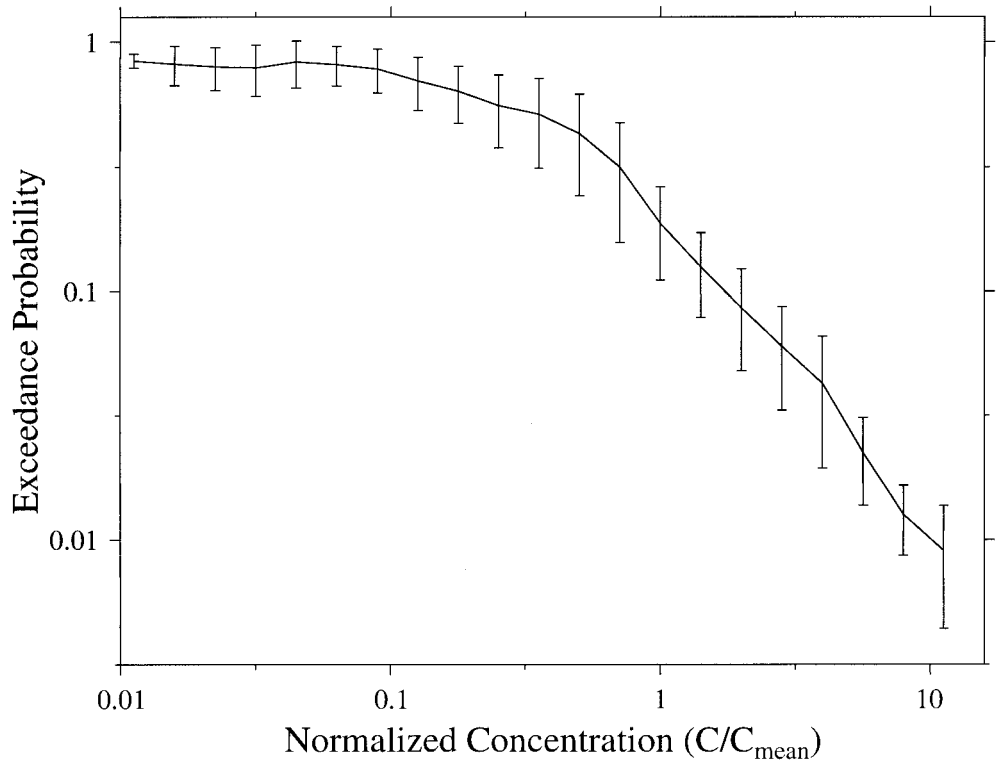

Fig. 13. Exceedance probability vs. concentration normalized to the local mean concentration. Centerline is the mean for all 61 data records; error bars indicate one standard deviation.

with olfactory-mediated search. Under field conditions, highly mobile animals such as blue crabs rarely pause while searching in response to chemical stimuli. Because an entire search path (1–3 m) may take only a few seconds to 1 min to traverse and locomotion is essentially continuous towards an odor source (Zimmer-Faust et al. 1995; Finelli 1997), there appears to be little averaging of chemosensory information in time or space. This situation may be quite different for less mobile organisms, such as echinoderms and gastropods; however, there is almost no information concerning the ability of such animals to navigate turbulent plumes, although it is clear that they respond to olfactory cues (Sloan and Northway 1982; Valentincic 1991; Moore and Lepper 1997).

At time scales more appropriate to animal sensory systems, turbulent odor plumes consist of discrete packets of odor separated by clean fluid (Murlis and Jones 1981). Under some laboratory conditions and the field conditions studied here, characteristics of these odor packets (e.g., peak slope, peak height) vary consistently within and between plumes (Figs. 9, 10) and, thus, have been suggested as directional cues for organisms (Moore and Atema 1988, 1991; Zimmer-Faust et al. 1988). Whether the fine-scale properties of odor packets provide information used by navigating organisms depends on the temporal response of olfactory neurons. For example, previous work on neurophysiological preparations of lobster chemosensory receptor cells has shown that discrete odor packets can be discriminated from each other at rates up to 4 Hz (Gomez et al. 1994). This rate also corresponds to the frequency at which lobsters sample odor plumes by flicking their antennules (i.e., sniffing) in behaviorally responding to chemical stimuli (Berg et al. 1992). Thus, lobsters may obtain information regarding the distance and direction of an odor source from the properties of individual odor pulses that arrive at rates up to 4 pulses s^{-1} (Gomez et al. 1994; Gomez and Atema 1996).

However, measurements of specific odor packet properties may require responses by chemosensory receptor cells at higher rates. For example, the rate of change in concentration within an odor filament (i.e., peak slope) has received considerable attention from previous investigators (Moore and Atema 1988, 1991; Zimmer-Faust et al. 1988). Given peak lengths on the order of 0.2–0.5 s (the range observed in our current field experiments), one-half of which is on the leading edge, animals would need to differentiate between peak slopes whose total durations (trough to peak) are 0.1–0.25 s. There is currently no evidence to show that any marine animal can (or cannot) measure the peak slope at this time scale. However, at least one experiment has shown that odor signals are integrated by lobster olfactory receptor cells over periods of 0.1–0.2 s (Gomez and Atema 1996). In addition to the lack of information regarding the temporal response of chemosensory neurons, a potential problem in linking odor packet properties to physiological properties is that studies of odor plumes (including our field experiment) have relied on stationary point measurements of odor concentration. As such, it is unclear whether odor packets and related properties (e.g., peak slope) will remain coherent as an organism the size of a lobster or blue crab moves through the fluid environment, as sensory structures including anten-

nules are driven through them at high speeds, or as respiratory currents modify the local flow field (Moore et al. 1994).

Unfortunately, our current knowledge of olfactory-mediated search is limited to correlative studies of animal behavior and a small number of plume measurements, and in marine systems our knowledge of the time scales over which peripheral and central nervous systems process and integrate chemosensory stimuli is limited to very few studies of crustacean chemoreceptor cells (Gomez et al. 1994; Gomez and Atema 1996). In addition, we know little about the extent to which odor stimuli are spatially averaged by populations of olfactory cells, by central nervous systems, or by physical processes (e.g., diffusional boundary layers; Cheer and Koehl 1988; Vogel 1983) that deliver odors to peripheral receptor neurons. Given our current limited knowledge linking the physics of plume dispersal and the physiology of odor reception, it is premature to assign a great deal of weight to any one measured odor packet parameter or chemosensory processing mechanism. Instead, our current field study shows that the distributions of the time-averaged concentration, odor packet properties, and conditional concentration statistics covary in space over a wide range of hydrodynamic conditions. The overall degree of similarity in these distributions suggests that animals may be able to rely on any number of covarying plume properties that show consistent near-Gaussian distributions. Moreover, we advocate the development of a more general understanding of odor plume dispersal based on combined physical and chemical measurements made at temporal and spatial scales relevant to peripheral and central nervous systems. An approach similar to the one used in our present study might provide new insights on odor packet properties, chemical signal intermittency, and odor plume meandering that can significantly increase understanding about the mechanisms that ultimately regulate odor-mediated search behavior by organisms within natural marine habitats.

References

ATEMA, J. 1996. Eddy chemotaxis and odor landscapes: Exploration of nature with animal sensors. Biol. Bull. **191:** 129–138.

——— AND D. ENGSTROM. 1971. Sex pheromone in the lobster *Homarus americanus.* Nature **232:** 261–263.

——— P. A. MOORE, L. P. MADIN, AND G. A. GERHARDT. 1991. Subnose-1: Electrochemical tracking of odor plumes at 900 m beneath the ocean surface. Mar. Ecol. Prog. Ser. **74:** 303–306.

BEACH, D. H., N. J. HANSCOMB, AND F. F. G. ORMOND. 1975. Spawning pheromone in crown-of-thorns starfish. Nature **254:** 135–136.

BERG, K., R. VOIGT, AND J. ATEMA. 1992. Flicking in the lobster *Homarus americanus*: Recordings from electrodes implanted in antennular segments. **183:** 377–378.

BOSSERT, W. H., AND E. O. WILSON. 1963. The analysis of olfactory communication among animals. J. Theor. Biol. **5:** 443–469.

BOUDREAU, B., E. BOURGET, AND Y. SIMARD. 1993. Behavioral responses of competent lobster postlarvae to odor plumes. Mar. Biol. **117:** 63–69.

BROWN, B., AND D. RITTSCHOF. 1984. Effects of flow and concentration of attractant on newly hatched oyster drills *Urosalpinx cinera* (Say). Mar. Behav. Physiol. **11:** 75–93.

CHEER, A. Y. L., AND M. A. R. KOEHL. 1988. Paddles and rakes: Fluid flow through bristled appendages of small organisms. J. Theor. Biol. **129:** 17–39.

CRISP, D. J., AND P. S. MEADOWS. 1962. The chemical basis of gregariousness in cirripedes. Proc. R. Soc. Lond. B **156:** 500–520.

DAVIDSON, M. J., K. R. MYLNE, C. D. JONES, J. C. PHILLIPS, R. J. PERKINS, J. C. H. FUNG, AND J. C. R. HUNT. 1995. Plume dispersion though large groups of obstacles—a field investigation. Atmos. Environ. **29:** 3245–3256.

DENNY, M. W. 1988. Biology and the mechanics of the wave-swept environment, 1st ed. Princeton Univ. Press.

———. 1993. Air and water. Princeton Univ. Press.

DUSENBURY, D. B. 1992. Sensory ecology: How organisms acquire and respond to information. Freeman.

FINELLI, C. M. 1997. The effects of behavior and physics on ecological processes. Ph.D. dissertation, Marine Science Program, Univ. of South Carolina-Columbia.

GLEESON, R. A. 1980. Pheromone communication in the reproductive behavior of the blue crab, *Callinectes sapidus.* Mar. Behav. Physiol. **7:** 119–134.

GOMEZ, G., AND J. ATEMA. 1996. Temporal resolution in olfaction: Stimulus integration time of lobster chemoreceptor cells. J. Exp. Biol. **199:** 1771–1779.

———, R. VOIGT, AND J. ATEMA. 1994. Frequency filter properties of lobster chemoreceptor cells determined with high-resolution stimulus measurement. J. Comp. Physiol. A **174:** 803–811.

HANNA, S. R., AND E. M. INSLEY. 1989. Time series analyses of concentration and wind fluctuations. Boundary-Layer Meteorol. **47:** 131–147.

HIMMELMAN, J. H. 1988. Movement of whelks (*Buccinum undatum*) towards a baited trap. Mar. Biol. **97:** 521–531.

HOROWITZ, P., AND W. HILL. 1989. The art of electronics, 2nd ed. Cambridge Univ. Press.

JENKINS, G. M., AND D. G. WATTS. 1968. Spectral analysis and its applications. Holden-Day.

KAIMAL, J. C., AND J. J. FINNIGAN. 1994. Atmospheric boundary layer flows. Oxford Univ. Press.

KLEEREKOPER, H., D. GRUBER, AND J. MATIS. 1975. Accuracy of localization of a chemical stimulus in flowing and stagnant water by the nurse shark, *Ginglymostoma cirratum.* J. Comp. Physiol. **98:** 257–275.

KOLMOGOROV, A. N. 1941. On degeneration of isotropic turbulence in incompressible viscous liquid. Dokl. Akad. Nauk SSSR **31:** 538–540.

KUENEN, L. P. S., AND R. T. CARDE. 1994. Strategies for recontacting a lost pheromone plume: Casting and upwind flight in the male gypsy moth. Physiol. Entomol. **19:** 15–29.

LIST, E. J. 1982. Turbulent jets and plumes. Annu. Rev. Fluid Mech. **14:** 189–212.

MATHEWSON, R. F., AND E. S. HODGSON. 1972. Klinotaxis and rheotaxis in orientation of sharks toward chemical stimuli. Comp. Biochem. Physiol. A **42:** 79–84.

MOORE, P. A., AND J. ATEMA. 1988. A model of a temporal filter in chemoreception to extract directional information from a turbulent odor plume. Biol. Bull. **174:** 355–363.

———, AND ———. 1991. Spatial information in the three-dimensional fine structure of an aquatic odor plume. Biol. Bull. **181:** 408–418.

———, G. A. GERHARDT, AND J. ATEMA. 1989. High resolution spatio-temporal analysis of aquatic chemical signals using microelectrochemical electrodes. Chem. Senses **14:** 829–840.

———, AND D. M. E. LEPPER. 1997. Role of chemical signals in the orientation behavior of the sea star *Asterias forbesi.* Biol. Bull. **192:** 410–417

———, M. J. WEISSBURG, J. M. PARRISH, R. K. ZIMMER-FAUST, AND G. A. GERHARDT. 1994. The spatial distribution of odors

in simulated benthic boundary layer flows. J. Chem. Ecol. **20:** 255–279.

MURLIS, J., AND C. D. JONES. 1981. Fine scale structure of odour plumes in relation to insect orientation to distant pheromone and other attractant sources. Physiol. Entomol. **6:** 71–86.

———, J. S. ELKINTON, AND R. T. CARDE. 1992. Odor plumes and how insects use them. Annu. Rev. Entomol. **37:** 505–532.

MYLNE, K. R. 1992. Concentration fluctuation measurements in a plume dispersing in a stable surface layer. Boundary-Layer Meteorol. **60:** 15–48

———, AND P. J. MASON. 1991. Concentration fluctuation measurements in a dispersing plume at a range of up to 1000 m. Q. J. R. Meteorol. Soc. **177:** 177–206.

NEVITT, G. A., R. R. VEIT, AND P. KAREIVA. 1995. Dimethyl sulphide as a foraging cue for Antarctic procellariiform seabirds. Nature **376:** 680–682.

PASQUILL, F., AND F. B. SMITH. 1983 Atmospheric diffusion, 3rd ed. Horwood.

PAWLIK, J. R. 1992. Chemical ecology of the settlement of benthic marine invertebrates. Oceanogr. Mar. Biol. Annu. Rev. **30:** 273–335.

PRESS, W. H., S. A. TEUKOLSKY, W. T. VETTERLING, AND B. P. FLANNERY. 1992. Numerical recipes in C, 2nd ed. Cambridge Univ. Press.

RITTSCHOF, D. 1980. Chemical attraction of hermit crabs and other attendants to simulated gastropod predation sites. J. Chem. Ecol. **6:** 103–118.

———. 1992. Chemosensation in the daily life of crabs. Am. Zool. **32:** 363–369.

SAS INSTITUTE. 1984. SAS user's guide, version 5 ed. SAS Institute.

SLOAN, N. A., AND S. M NORTHWAY. 1982. Chemoreception by the asteroid *Crossaster papposus.* J. Exp. Mar. Biol. Ecol. **61:** 85–98.

SWEATMAN, H. 1988. Field evidence that settling coral reef fish larvae detect resident fishes using dissolved chemical cues. J. Exp. Mar. Biol. Ecol. **124:** 163–174.

SZIGALY, J., G. G. KATUL, M. B. PARLANGE, J. D. ALBERTSON, AND A. T. CAHILL. 1996. The local effect of intermittency on the inertial subrange energy spectrum of the atmospheric surface layer. Boundary-Layer Meteorol. **79:** 35–50.

VALENTINCIC, T. 1991. Behavioral responses of the brittle star *Ophiura ophiura* to amino acids, acetylcholine and related low-molecular-weight compounds. Chem. Senses **16:** 251–266.

VOGEL, S. 1983. How much air passes through a silkmoth's antenna? J. Insect Physiol. **29:** 597–602.

———. 1994. Life in moving fluids, 2nd ed. Princeton Univ. Press.

WEISSBURG, M. J., AND R. K. ZIMMER-FAUST. 1993. Life and death in moving fluids: Hydrodynamic effects on chemosensory-mediated predation. Ecol. **74:** 1428–1443.

———, AND ———. 1994. Odor plumes and how blue crabs use them in finding prey. J. Exp. Biol. **197:** 349–375.

WOODIN, S. A. 1991. Recruitment of infauna: Positive or negative cues? Am. Zool. **31:** 797–807.

WOODWARD, F. I., AND J. E. SHEEHY. 1983. Principles and measurements in environmental biology. Butterworth.

WRIGHT, R. H. 1958. The olfactory guidance of flying insects. Can. Entomol. **90:** 81–89.

YEE, E. 1990. The shape of the probability density function of short-term concentration fluctuations of plumes in the atmospheric boundary layer. Boundary-Layer Meteorol. **51:** 269–298.

———, P. R. KOSTENIUK, G. M. CHANDLER, C. A. BILTOFT, AND J. F. BOWERS. 1993*a*. Statistical characteristics of concentration fluctuations in dispersing plumes in the atmospheric surface layer. Boundary-Layer Meteorol. **65:** 69–109.

———, D. J. WILSON, AND B. W. ZELT. 1993*b*. Probability distributions of concentration fluctuations of a weakly diffusive passive plume in a turbulent boundary layer. Boundary-Layer Meteorol. **64:** 321–354.

ZIMMER-FAUST, R. K., FINELLI, C. M., PENTCHEFF, N. D., AND D. S. WETHEY. 1995. Odor plumes and animal navigation in turbulent water flow: A field study. Biol. Bull. **188:** 111–116.

———, AND E. SPANIER. 1987. Gregariousness and sociality in spiny lobsters: Implications for den habitation. J. Exp. Mar. Biol. Ecol. **105:** 57–71.

———, J. M. STANFILL, AND S. B. COLLARD III. 1988. A fast, multichannel fluorometer for investigating aquatic chemoreception and odor trails. Limnol. Oceanogr. **33:** 1586–1595.

Received: 9 February 1998
Accepted: 25 January 1999
Amended: 8 February 1999